cigre Turkey

TEPES
TURKISH JOURNAL OF ELECTRICAL POWER AND ENERGY SYSTEMS

TEPES, Vol. 2, Issue. 1, 58-65, 2022 **DOI:** 10.5152/tepes.2022.21014

RESEARCH ARTICLE

Transformer-Less Single-Stage and Single-Switched PI-Controlled AC-DC Converter Design for Automotive Applications

Davut Ertekin[1], Mesut Berke Bilgiç[2], Bülent Mutlu[2]

[1]Department of Electrical and Electronics Engineering, Bursa Technical University, Bursa, Turkey
[2]Valeo Automotive Industry and Trade Inc. (Valeo Otomotiv Sanayi ve Ticaret A.Ş.), Bursa, Turkey

Cite this article as: D. Ertekin, M. B. Bilgiç & B. Mutlu. Transformer-less single-stage and single-switched PI-controlled AC-DC converter design for automotive applications. *Turk J Electr Power Energy Syst*, 2022; 2(1): 58-65.

ABSTRACT

Alternators are electro-mechanical types of equipment that can convert mechanical energy to electrical energy. These devices frequently are used in automotive industries. Therefore, it is important to test them before being assembled on the automobiles for increasing reliability. In this study, a transformer-less single-stage and single-switched alternating current-direct current converter structure is proposed in order to test the operation quality of the alternator. By using the proportional integral controller, a constant output voltage is provided at three different voltage levels. This is done since different test voltages are requested by the consumers as different alternators with different operational voltages are available in the industry. In addition, since no transformer is used in the proposed structure, the volume and production cost of the converter are appropriate. In this study, the proposed converter and the controller system are analyzed in Matlab/SIMULINK environment. In the analysis, it was seen that the proposed converter works with proper efficiency.

Index Terms—AC-DC converter, PI controller, power factor correction (PFC), full-wave rectifier

I. INTRODUCTION

In the automotive sector, alternating current generators that provide energy to motor vehicles by converting mechanical energy into electrical energy are called alternators. Alternators in automobiles charge the battery while the vehicle's engine run. Thus, they contribute to the feeding of the equipment of the vehicle that needs electricity. To activate the internal circuits of the alternator, a direct current (DC) voltage is requested. There are different types of alternators that need different operational voltages. Therefore, in order to test the performance and working quality of the alternator, the test equipment should work under different voltages. This means the test converter circuit should generate different voltages that will apply as the input voltages for the alternators [1-4].

Alternating current-direct current (AC-DC) converters used in many power electronic devices typically consist of an AC-DC rectifier connected in series with a DC-DC converter. The AC-DC rectifier converts the AC voltage at the input to a DC voltage. Then, the DC-DC converter provides the desired DC voltage at the output. Single-stage AC-DC converters are widely used due to their simplicity and low cost [5-7]. For applications requiring low output voltage, the power conversion process results in low efficiency due to the voltage difference at the input and output [8-10]. To avoid this, a high-stage transformer should be used in the circuit. The inclusion of the transformer in the circuit increases the number of components, the volume of the circuit, and the cost of manufacture. In addition, the efficiency is considerably reduced due to transformer leakage inductance [11-13].

Apart from that, boost-based power factor correction (PFC) is insufficient to provide short-circuit protection at the output and to limit the inrush current at the input. By using a Buck-based PFC circuit, these disadvantages can be reduced.

Different structures for regulating the bus-bar voltage are available in the literature [14-17]. Since transformers are used in the converters suggested in [18], leakage inductance cannot be avoided. This increases the voltage stress on the semiconductor elements and reduces the conversion efficiency [19, 20]. For the converters with more than one switch, the control process is difficult and complex.

In this study, a proportional integral (PI)-controlled AC-DC buck converter is proposed. As a controller, the PI controller structure is preferred due to its simplicity and high efficiency. By adjusting the duty cycle (D) of the active switch in the circuit, it provides a constant

Corresponding author: Davut Ertekin, davood.ghaderi@btu.edu.tr

Received: February 16, 2022
Accepted: March 12, 2022

output voltage at three different levels (10 V, 13.5 V, and 18 V) for variable input voltages. By generating different voltages, the proposed converter can be used to test the performance quality of different alternator types since different operational voltages can be requested by the customers. It means different alternators are available in the automotive industries that can work with 10 V, 13.5 V, or other voltages.

A step-down transformer is not used in the proposed converter to achieve low voltage levels. İnstead, a full-wave rectifier converter is used that can correct the power factor since, in the full-wave rectifier, the average current in the input source is zero. Therefore, it can avoid the problems associated with non-zero average source currents, especially in transformers. The output of the full-wave rectifier has inherently less ripple than the half-wave rectifier.

At the same time, the volume of the circuit and the production cost are considerably reduced by using the minimum number of elements. However, since only one active switch is used, the control process and the analysis of the circuit are significantly simplified.

This paper aimed to verify the performance of the proposed AC-DC converter and is organized as follows: the converter structure proposed in chapter 2 presents the different operating modes of the converter, PI controller calculations, and continuous current mode (CCM) analysis. The calculation of component values is presented in chapter 3, and the simulation results are shown in chapter 4. Finally, in chapter 5, the results obtained and explanations about the results are included.

II. PROPOSED CONVERTER

The proposed single-stage AC-DC converter is shown in Fig. 1. The circuit basically consists of a rectifier and a buck converter. Components D_1–D_4 constitute the bridge rectifier and S, L, D_5, and C_o form the buck converter. It has 2 Ω and 2 mH resistor–inductor load connected in series as load. This amount of the load is based on the practical alternator internal resistor and inductor values.

In the bridge rectifier, the D_1 and D_4 diodes conduct together, and the D_2 and D_3 diodes transmit simultaneously and in the time intervals when the D_1–D_4 pair is open. In the loop with D_1, D_2, and the source, Kirchhoff's law of voltages shows that D_1 and D_2 cannot be on at the same time. Similarly, D_3 and D_4 cannot transmit at the same time. The load current can be positive but never zero. Switch S is controlled by a PI controller, driven by a pulse width modulated (PWM) signal with T as the time period and D as the duty cycle. The requested output voltage can be obtained by adjusting the duty cycle of the switch in the range of 0–1.

Main Points

- Presenting a AC-DC converter for alternator tests in automotive industries.
- Presenting a single-switched and single-stage topology.
- Simple control method with wide range of output voltages.
- Efficient and simple to be implemented.

In the CCM, the proposed converter can be examined in two conduction and cut-off modes when the power switch is on and off, respectively. The states of the components used in the converter are analyzed separately for each mode. Fig. 2 and Fig. 3 show the circuit structure for the on and off modes. Fig. 4 shows the waveforms of the elements in CCM operation.

Mode 1 [0 – DT]: In this time interval, switch S is on and inductor L is charging through capacitor C_1. Since the D_5 diode is reverse biased, the voltage on it becomes zero and operates in the cut-off state. The load current is provided by the output capacitor C_o. In this study, the voltage on the load is named V_o and the voltage on the capacitor C_1 is named V_{in}. The equations for this operating mode are as follows:

$$V_L = V_{in} - V_o = L\frac{di_L}{dt} \tag{1}$$

$$V_{D_5} = V_{in} \tag{2}$$

The ripple in current when the switch is closed is calculated as:

$$\frac{di_L}{dt} = \frac{\Delta i_L}{\Delta t} = \frac{\Delta i_L}{DT} = \frac{V_{in} - V_o}{L} \tag{3}$$

$$(\Delta i_L)_{kapal1} = \left(\frac{V_{in} - V_o}{L}\right)DT \tag{4}$$

Mode 2 [DT – T]: Switch S is in off state during this time interval. When the switch is deactivated, the diode D_5 becomes forward biased to conduct the inductor current, therefore easily it can be seen that the circuit in Fig. 3 is valid. The equations for this operating mode are as follows:

$$V_L = -V_o = L\frac{di_L}{dt} \tag{5}$$

The ripple in current when the switch is open is calculated as:

$$\frac{\Delta i_L}{\Delta t} = \frac{\Delta i_L}{(1-D)T} = \frac{-V_o}{L} \tag{6}$$

$$(\Delta i_L)_{açık} = \left(\frac{-V_o}{L}\right)(1-D)T \tag{7}$$

In steady-state operation, the amplitude of the current ripple for both on and off states are the same and the net change in inductor current over a period is zero. In that case,

$$(\Delta i_L)_{kapal1} + (\Delta i_L)_{açık} = 0 \rightarrow \left(\frac{V_{in} - V_o}{L}\right)DT - \left(\frac{V_o}{L}\right)(1-D)T \tag{8}$$

By a simplification in (8), the output voltage can be calculated as below:

$$V_o = V_S D \tag{9}$$

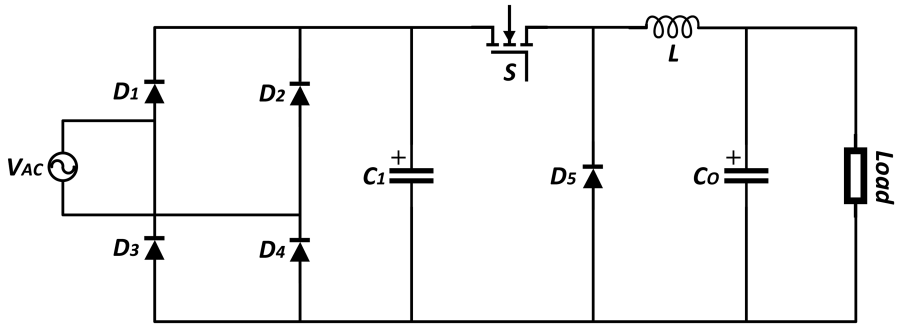

Fig. 1. Circuit diagram of the proposed AC-DC converter.

This equation simply can show that the applied converter can act like a buck converter and decrease the input DC voltage across the capacitor C_1. For the next step, it is important to present a controller to prepare the required pulse to the switch for generating smaller voltages for the alternator as the load.

A. PI Controller and Small-Signal Analysis

The first thing to do for a system to be controlled is to perform the system modeling. Modeling the converter to be realized in power electronics circuits provides a correct understanding of the open-closed loop control response of the converter.

The PI controller provides the control process using the error input and historical error signals. In the PI controller, the reference voltage and the output voltage are compared, and then the sampled voltage passes through the controller, and controller output is compared with the inductor current to obtain the D of the PWM signal. Therefore, the converter provides the requested output voltage [11]. Fig. 5 shows the mathematical model of the pro posed PI controller.

By looking at the state space form of the system to be controlled, it is seen that it has multiple inputs/outputs and state variables. If we express the system in a simple form consisting of one input and one output, the input of the system can be shown as D and the output of the system as *Vo*.

In order to write the single input and single output model in the state space form according to the determined state variables, the state and the output equations should be obtained:

$$\frac{dx(t)}{dt} = Ax + Bu \quad \text{State equation}$$
$$y(t) = Cx \quad \text{Output equation} \tag{10}$$

To obtain the state space model of the Buck converter, the state equations for the state variables need to be obtained. If we obtain the generalized expressions from the equations of inductor current and capacitor voltage in both operating ranges, the inductor current can be calculated:

$$\frac{di_L(t)}{dt} = \frac{1}{L}\left[\left(V_{in} - V_o(t)\right)D + \left(-V_c(t)\right)(1-D)\right] \rightarrow \frac{di_L(t)}{dt} = \frac{V_{in}}{L}D - \frac{V_0(t)}{L} \tag{11}$$

The voltage equation for the output capacitor can be obtained by:

$$\frac{dv_o(t)}{dt} = \frac{1}{C}\left[\left(i_L(t) - \frac{V_0(t)}{R}\right)D + \left(i_L(t) - \frac{V_0(t)}{R}\right)(1-D)\right] \rightarrow \frac{dv_o(t)}{dt} = \frac{1}{C}i_L(t) - \frac{V_0(t)}{RC} \tag{12}$$

The state space form of the system can be written by controlling it with the differential equations we have obtained for the state variables:

$$x_1(t) = i_L(t) \tag{13}$$

$$x_2(t) = v_c(t) \tag{14}$$

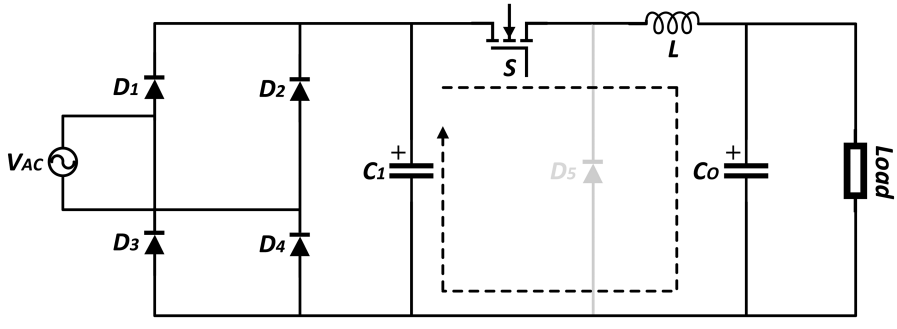

Fig. 2. Circuit structure for the conduction mode of the switch.

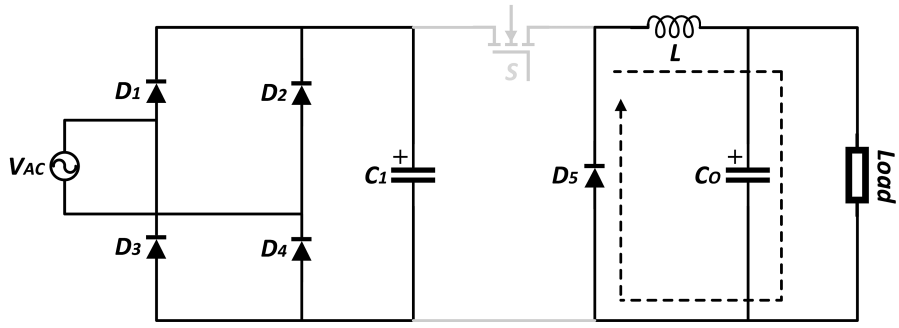

Fig. 3. Circuit structure for the cut mode of the switch.

$$\frac{dx_1(t)}{dt} = -\frac{1}{L}x_2 + \frac{V_{in}}{L}u \text{ 1st state equation} \quad (15)$$

$$\frac{dx_2(t)}{dt} = \frac{1}{C}x_1 - \frac{1}{RC}x_2 \text{ 2nd state equation} \quad (16)$$

The state space form for the buck converter part:

$$\frac{d}{dt}\begin{bmatrix} x_1(t) \\ x_2(t) \end{bmatrix} = \begin{bmatrix} 0 & -\frac{1}{L} \\ \frac{1}{C} & -\frac{1}{RC} \end{bmatrix}\begin{bmatrix} x_1(t) \\ x_2(t) \end{bmatrix} + \begin{bmatrix} \frac{V_{in}}{L} \\ 0 \end{bmatrix}u(t) \quad (17)$$

$$y(t) = \begin{bmatrix} 0 & 1 \end{bmatrix}\begin{bmatrix} x_1(t) \\ x_2(t) \end{bmatrix} \quad (18)$$

The transfer function can be found by writing the equations of state we have obtained for the Buck converter in the S-space:

$$sX_1 = -\frac{1}{L}Y(s) + \frac{V_{in}}{L}U(s) \quad (19)$$

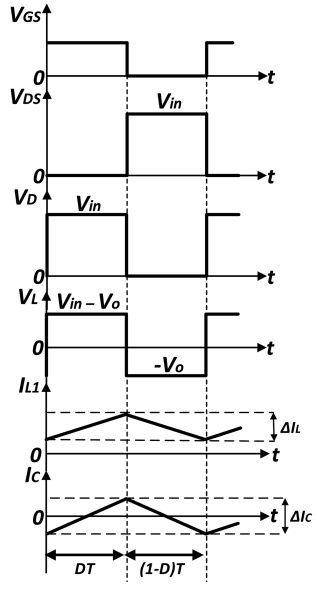

Fig. 4. Converter waveforms in CCM operational mode.

$$sY(s) = \frac{1}{C}X_1 - \frac{1}{RC}Y(s) \quad (20)$$

If X_1 is subtracted from Equation 20 and replaced in Equation 19:

$$G_p(s) = \frac{Y(s)}{U(s)} = \frac{\frac{V_{in}}{LC}}{s^2 + \frac{1}{RC}s + \frac{1}{LC}} \quad (21)$$

If the open-loop response of the system is examined, it is seen that it has a damped form by a low damping ratio (ξ). By designing a controller with a classical PI controller to control the output of the buck converter, the output voltage can be controlled. In this case, the transfer function of the PI controller will be as follows:

$$G_c(s) = K_p + \frac{K_i}{s} \quad (22)$$

In this case, the closed-loop transfer function of the system becomes:

$$\text{Closed Loop Transfer Function} \rightarrow \frac{\frac{V_{in}}{LC}K_p s + \frac{V_{in}}{LC}K_i}{\frac{1}{RC}s^2 + \left(\frac{1}{LC} + \frac{V_i}{LC}K_p\right)s + \frac{V_i}{LC}K_i} \quad (23)$$

III. CALCULATION OF COMPONENT VALUES

While designing the converter circuit, it was assumed that the converter was in a stable state and the semiconductor switching elements were considered ideal, and the losses of the inductor and capacitors were neglected. It is also assumed that the converter works in the CCM.

For the converter circuit shown in Fig. 1, the relationship between V_o and V_s voltages in steady state is as shown in Equation 9. It can be rewritten as:

$$D = \frac{V_o}{V_{in}} = \frac{t_{on}}{T} \quad (24)$$

Here, D is the duty cycle, t_{on} is the switch's conduction time, and T is the switching period.

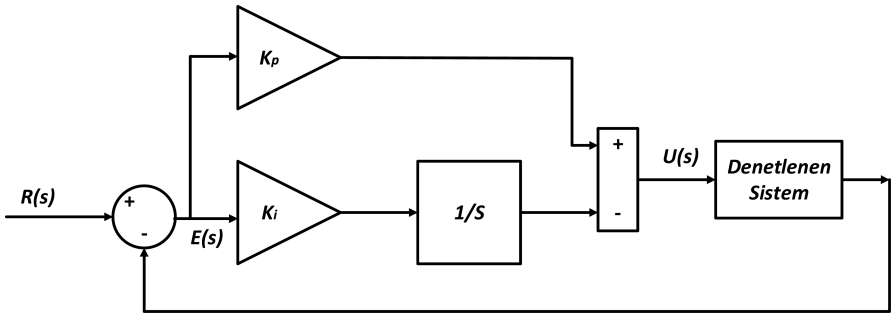

Fig. 5. Mathematical model of the PI controller.

The following equations are used to calculate the minimum inductor and capacitor values in the circuit:

$$L = \frac{(1-D)R}{2f} \tag{25}$$

$$C_o = \frac{1-D}{8L(\Delta V_o / V_o)f^2} \tag{26}$$

These values are the minimum required component values. The component values used in the simulation and the designed circuit are shown in Table I.

IV. SIMULATION RESULTS

This section shows the results of the simulation for the proposed converter and controller circuits. The simulation of the circuit was carried out in Matlab/SIMULINK environment. In Fig. 6, the input voltage with 220 V_{rms} and 50 Hz frequency and the desired output voltage at three different levels are shown. Three different voltages are planned to be obtained. These voltages are 10, 13.5, and 18 VDC voltages that are the industrial and requested real DC voltages. The desired constant output voltage is achieved rapidly at 10 V and 18.5 V values of the output voltage. After a very small delay of 0.3 s for 13.5 V, the desired output voltage is achieved. Since this delay time is very short, it will not have a negative effect on the system, especially by considering the fact that the proposed converter should generate these voltages for a long time for test purposes.

TABLE I.
COMPONENT VALUES USED IN THE CIRCUIT

Parameters	Value
Input AC voltgae V_{AC}	220 V_{rms}
Output DC voltage V_o	8, 13.5 ve18 V
Inductor L	100 µH
Capacitor C_o	2200 µF
Capacitor C_1	2200 µF
Switching frequency f_s	20 kHz
Load (alternator)	2 Ω, 2 mH

Fig. 7 shows the waveforms of the output current and voltage. One can see from the figure that the output current changes at three different levels immediately when the output voltage changes.

Fig. 8 shows the voltage and current waveforms for the power switch. As can be seen, there is a voltage of approximately 300 V on the switch during the cut-off time duration and the switch current is zero in this time interval. For the times the switch is in operation, 6 A current flows on the switch and the voltage on it is zero since the switch behaves like a short circuit. In addition, the simulation result also confirms the graph shown in Fig. 4. Fig. 9 shows the voltage waveform for the buck converter's diode, D_5. As can be seen from the figure, when the diode is conducting, the voltage on it is zero. During the cut-off time duration, there is a voltage of about 300 V on this diode. These DC voltages approximately are the peak voltage of the input AC voltage. The power diodes in industrial applications can withstand these voltages easily.

V. CONCLUSION

In this study, a transformer-less single-switch AC-DC converter structure is investigated for test application in automotive industries. The proposed structure can convert and transfer the grid voltage into three different (10, 13.5, and 18 VDC) constant voltage levels at the output for applying to the alternator to investigate the reaction of this device before assembling on the automobile. The ripple in output current and voltage is quite low which is a requested parameter for better analysis of the alternator for probably fault detection investigations. The PI controller structure is preferred as the controller in the converter due to its simple, fast response, and low-cost features. Compared to other structures, its specifications such as the low number of components and the absence of transformers that increase the volume and cost of the circuit make the recommended AC-DC buck converter preferred over other converters. After the circuit was analyzed mathematically in CCM, it was designed using the Matlab/SIMULINK package program and the results confirmed the theoretical analysis.

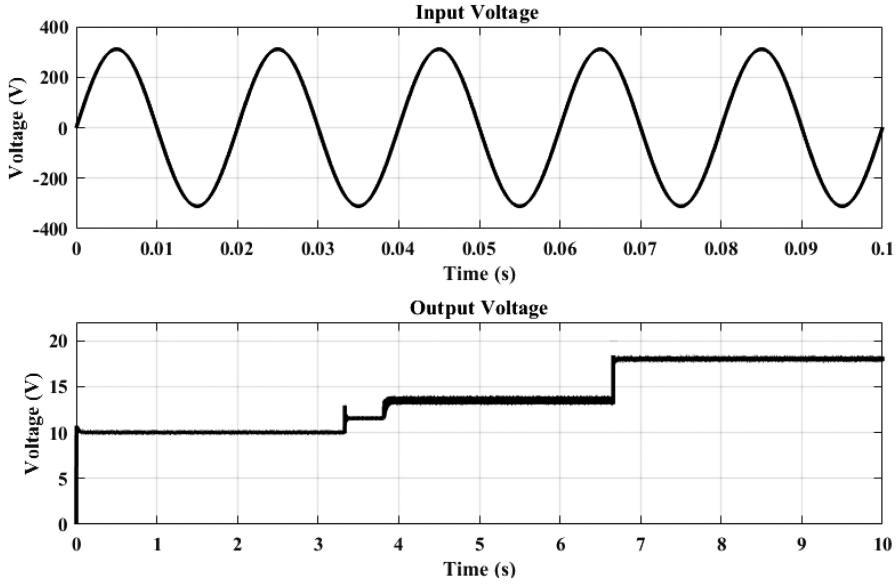

Fig. 6. Input and output waveforms of the converter.

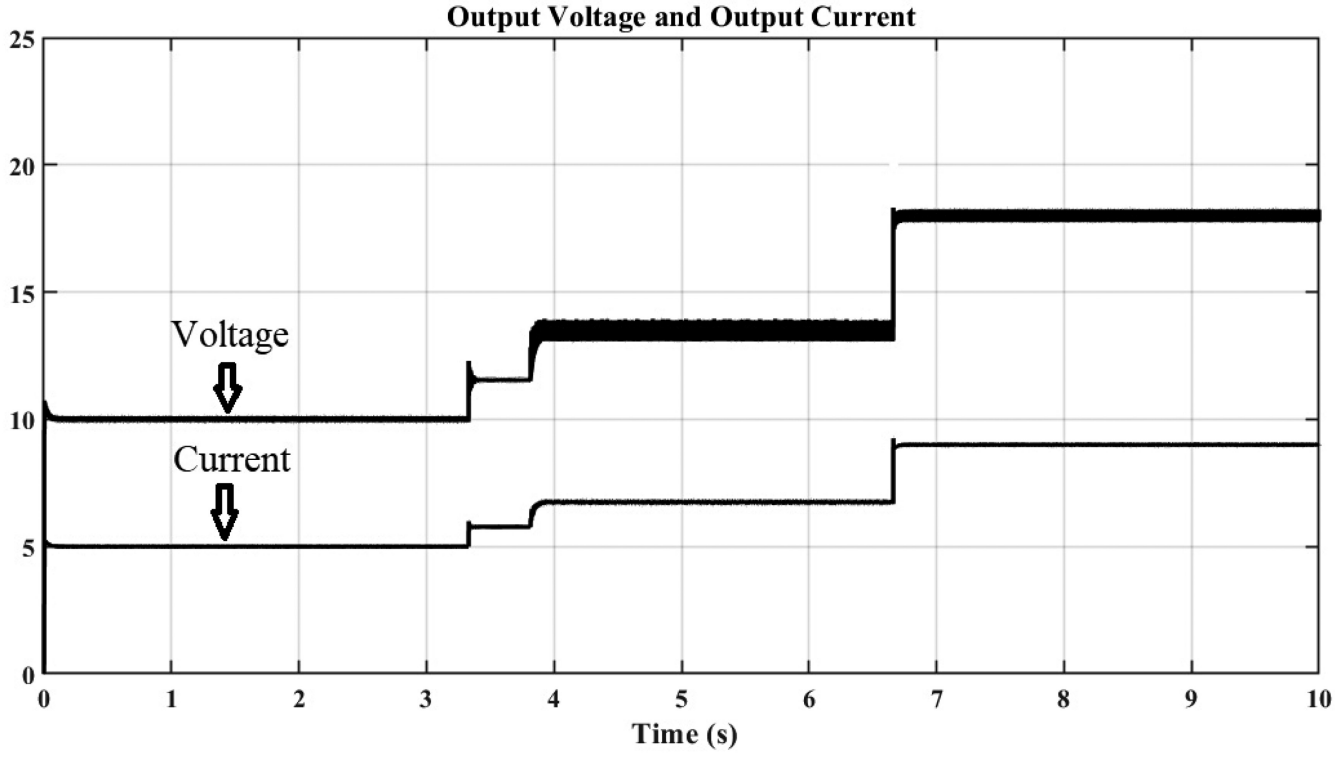

Fig. 7. Output voltage and current waveforms.

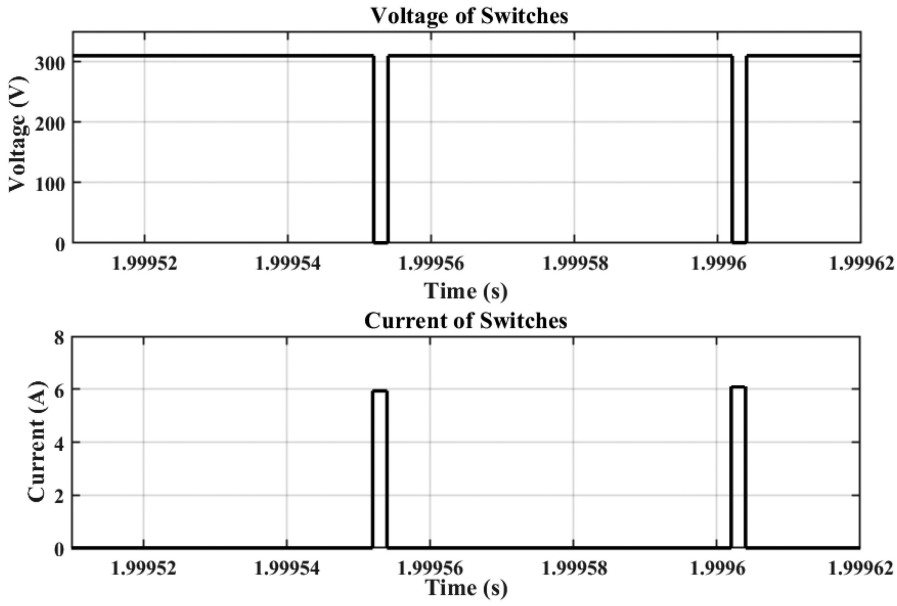

Fig. 8. Waveforms of switch's current and voltage.

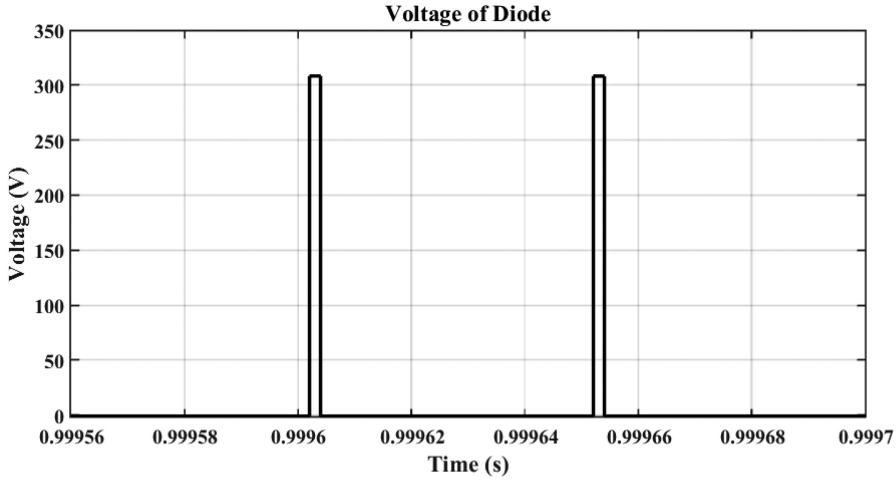

Fig. 9. Voltage waveform for diode D_5.

Peer-review: Externally peer-reviewed.

Acknowledgments: This study has been done as a part of R&D project between the Asst. Prof. Dr. Davut Ertekin from Bursa Technical University and Valeo Automotive Industry and Trade Inc. Bursa, under project untitled: Analog Controlled AC-DC Converter Design for Alternator Tests.

Declaration of Interests: The authors have no conflicts of interest to declare.

Funding: This project is supported by Valeo Automotive Industry and Trade Inc. Bursa, under the project entitled: Analog Controlled AC-DC Converter Design for Alternator Tests.

REFERENCES

1. D. Sarafianos, D. X. Llano, S. S. Ghosh, R. A. McMahon, S. Pickering, and T. J. Flack, "Control strategy for a multiphase Lundell-Alternator/Active -Rectifier system in 14 V automotive power systems," *IEEE Trans. Transp. Electrif.*, vol. 5, no. 2, pp. 347–355, 2019. [CrossRef]
2. S. Wu, S. Zuo, X. Wu, F. Lin, H. Zhong, and Y. Zhang, "Vibroacoustic prediction and mechanism analysis of claw pole alternators," *IEEE Trans. Ind. Electron.*, vol. 64, no. 6, pp. 4463–4473, 2017. [CrossRef]
3. C. -S. Yu, Y. -C. Lin, and C. -J. Chen, "Rotational speed detection for the automotive alternator with low loss rectifier in self-start," *IEEE Trans. Veh. Technol.*, vol. 70, no. 7, pp. 6514–6526, 2021. [CrossRef]

4. S. Wu, S. Zuo, and Y. Zhang, "Optimization for electromagnetic noise reduction in claw pole alternator by rotor claw chamfering," *IEEE Trans. Ind. Electron.*, vol. 65, no. 12, pp. 1–1, 2018. [CrossRef]
5. H. Wu, Y. Jia, F. Yang, L. Zhu, and Y. Xing, "Two-stage isolated bidirectional DC–AC converters with three-port converters and two DC buses," *IEEE J. Emerg. Sel. Top. Power Electron.*, vol. 8, no. 4, pp. 4428–4439, 2020. [CrossRef]
6. H. Wu, M. Han, and K. Sun, "Dual-voltage-rectifier-based single-phase AC–DC converters with dual DC bus and voltage-sigma architecture for variable DC output applications," *IEEE Trans. Power Electron.*, vol. 34, no. 5, pp. 4208–4222, 2019. [CrossRef]
7. S. A. Q. Mohammed, and J. -W. Jung, "A state-of-the-art review on soft-switching techniques for DC–DC, DC–AC, AC–DC, and AC–AC power converters," *IEEE Trans. Ind. Inform.*, vol. 17, no. 10, pp. 6569–6582, 2021. [CrossRef]
8. D. Ertekin, S. Padmanaban, P K. Maroti, B. Papari, and J. Bo HolmNielsen, "Design and implementation of an improved sinusoidal controller for a two-phase enhanced impedance source boost inverter," *Computers Electrical Engineering*, vol. 83, no. 3, pp. 1–18, 2020.
9. D. Hu, A. Yin, and D. ERTEKİN, "A transformer-less single-switch boost converter with high-voltage gain and mitigated-voltage stress applicable for photovoltaic utilizations," *Int. Trans. Electr. Energy Syst.*, vol. 30, no. 10, pp. 1–22, 2020. [CrossRef]
10. K. Bulut, and D. Ertekin, "Maximum power point tracking by the small-signal-based PI and Fuzzy logic controller approaches for a two-stage switched-capacitor DC-DC power boost converter applicable for photovoltaic utilizations," *El-Cezeri Fen ve Mühendislik Dergisi*, vol. 2020, no. 3, pp. 1167–1190, 2020.
11. S. Du, and B. Wu, "A transformerless bipolar modular multilevel DC–DC converter with wide voltage ratios," *IEEE Trans. Power Electron.*, vol. 32, no. 11, pp. 8312–8321, 2017. [CrossRef]
12. S. Du, B. Wu, and N. R. Zargari, "A transformerless high-voltage DC–DC converter for DC grid interconnection," *IEEE Trans. Power Deliv.*, vol. 33, no. 1, pp. 282–290, 2018. [CrossRef]
13. S. Du, B. Wu, D. Xu, and N. R. Zargari, "A transformerless bipolar multistring DC–DC converter based on series-connected modules," *IEEE Trans. Power Electron.*, vol. 32, no. 2, pp. 1006–1017, 2017. [CrossRef]
14. Y. -T. Huang, C. -H. Li, and Y. -M. Chen, "A modified asymmetrical half-bridge flyback converter for step-down AC–DC applications," *IEEE Trans. Power Electron.*, vol. 35, no. 5, pp. 4613–4621, 2020. [CrossRef]
15. M. Ryu, J. Baek, J. Kim, S. Park and H. Kim, "Electrolytic capacitor-less, non-isolated PFC converter for high-voltage LEDs driving," *8th International Conference on Power Electronics - ECCE Asia*, pp. 499–506, 2011. [CrossRef]
16. Y. Cai, J. Xu, P. Yang, J. Wu, and J. Sha, "Evaluation and suppression of a low-frequency output voltage ripple of a single-stage AC–DC converter based on an output impedance model," *IEEE Trans. Ind. Electron.*, vol. 66, no. 4, pp. 2803–2813, 2019. [CrossRef]
17. C. Chang, C. Cheng, E. Chang, H. Cheng, and B. Yang, "An integrated high-power-factor converter with ZVS transition," *IEEE Trans. Power Electron.*, vol. 31, no. 3, pp. 2362–2371, 2016. [CrossRef]
18. E. H. Ismail, A. J. Sabzali, and M. A. Al-Saffar, "Buck boost-type unity power factor rectifier with extended voltage conversion ratio," *IEEE Trans. Ind. Electron.*, vol. 55, no. 3, pp. 1123–1132, 2008. [CrossRef]
19. P. Das, A. Mousavi, and G. Moschopoulos, "An ac-dc single-stage full-bridge PWM converter with bridgeless input," IEEE Energy Convers. Congress and Exposition, vol. 2009, 2009, pp. 1347–1352. [CrossRef]
20. K. K. H. Dia, M. A. Choudhury, and Ahammad, "A single phase differential Zeta rectifier-inverter," *IEEE International WIE Conference on Electrical and Computer Engineering (WIECON-ECE)*, vol. 2015, pp. 284–288, 2015. [CrossRef]